CHITOSAN-CELLULOSE COMPOSITE MATERIALS: PREPARATION, CHARACTERIZATION AND APPLICATION FOR REMOVAL OF MICROCYSTIN

Chieu D. Tran[a,*], **Simon Duri**[a], **Ambra Delneri**[b], and **Mladen Franko**[b]

[a]Department of Chemistry, Marquette University, P. O. Box 1881, Milwaukee, WI 53201, USA

[b]Dept. of Environmental and Physical Chemistry, Nova Gorica University, Nova Gorica, Slovenia

Abstract

We developed a simple and one-step method to prepare biocompatible composites from cellulose (CEL) and chitosan (CS). [BMIm+Cl−], an ionic liquid (IL), was used as a green solvent to dissolve and prepare the [CEL+CS] composites. Since majority (>88%) of IL used was recovered for reuse by distilling the aqueous washings of [CEL+CS], the method is recyclable. XRD, FTIR, NIR, ^{13}C CP-MAS-NMR and SEM were used to monitor the dissolution and to characterize the composites. The composite was found to have combined advantages of their components: superior mechanical strength (from CEL) and excellent adsorption capability for microcystin-LR, a deadly toxin produced by cyanobacteria (from CS). Specifically, the mechanical strength of the composites increased with CEL loading; e.g., up to 5X increase in tensile strength was achieved by adding 80% of CEL into CS. Kinetic results of adsorption confirm that unique properties of CS remain intact in the composite, i.e., it is not only a very good adsorbent for microcystin but also is better than all other available adsorbents. For example, it can adsorb 4X times more microcystin than the best reported adsorbent. Importantly, the microcystin adsorbed can be quantitatively desorbed to enable the composite to be reused with similar adsorption efficiency.

Keywords

Cellulose; Chitosan; Ionic Liquid; Green Chemisty; Cyanotoxins; Microcystins

1. INTRODUCTION

Microcystin LR, produced by cyanobacteria, is one of the most deadly toxins present in drinking water [1–4]. At least 40 species of cyanobacteria release toxic cyanotoxins into water during algal blooms. Microcystins (MCs) are the most prevalent class of cyanotoxins. The MCs are very soluble in water and consist of over 80 reported variants; however, four MCs (LR, RR, LA, and YR (See Scheme 1 for structures) are of special concern to the Environmental Protection Agency (EPA) and are on EPA Contaminant Candidate List III. The World Health Organization (WHO) has set a provisional drinking water guideline of 1 µg/L for MC-LR. The toxicity of MCs is due to their strong binding and inhibition of protein

*Corresponding author: Tel: +01 424 288 5428; Fax: +01 288 7066 chieu.tran@marquette.edu.

phosphatases. MCs are also known to promote the growth of tumors; have a genotoxic effect as well as strong mutagenicity [1–4].

The presence of toxic cyanobacterial blooms in drinking water reservoirs may represent serious health risks for the human population. Considerable efforts have, therefore, been made to develop removal methods. Limited success has been made by use of such adsorbents as activated carbon, oxidation by ozone and chlorine dioxide, TiO_2 photocatalysis and ultrasonic irradiation [1–4]. Since these techniques cannot effectively remove the toxins in water, it is of particular importance that an effective removal technique based on the use of a biocompatible material be developed.

Chitosan (CS) is a linear amino polysaccharide, obtained by N-deacetylation of chitin, and chitin, which is found in the exoskeletons of crustaceans (e.g., crabs and shrimp), is the second most abundant naturally occurring polysaccharide [5–8]. CS has been a subject of intense studies for many years [9–24]. The popularity stems from the fact that it is biodegradable, biocompatible, and possesses unique structure and properties which have been successfully exploited in many applications including hemostasis, wound healing, bactericide and fungicide, drug delivery and adsorbent for organic and inorganic pollutants [9–29]. Of particular interest are reports that CS, when modified with fly ash or immobilized on clay, can adsorb and remove algae such as *Chlorella Pyrenoidosa* or *Microcystis Aeruginosa* in water [30–35]. Unfortunately, in spite of its potentials, there are drawbacks which severely limit applications of CS. For example similar to cellulose (CEL), the most abundant substance on earth, in CS, a network of intra- and inter-hydrogen bonds enables it to adopt an ordered structure [6–8]. While such structure is responsible for CS to have aforementioned properties and CEL to have superior mechanical strength, it also makes them insoluble in most solvents [6–8]. As a consequence, high temperature and strong exotic solvents such as methylmorpholine-N-oxide, dimethylthexylsilyl chloride or LiCl in dimethylacetamide (DMAc) are needed to dissolve CEL whereas an acid such as acetic acid is required to protonate amino groups of CS to facilitate its dissolution in water [6–29]. These methods are undesirable because they are based on the use of corrosive and volatile solvents, require high temperature and suffer from side reactions and impurities which may lead to changes in structure and properties of the polysaccharides. More importantly, it is not possible to use a single solvent or system of solvents to dissolve both CEL and CS. Furthermore, CS is known to swell in water which leads to structural weakening in wet environments [6–21]. To increase the structural strength of CS products, attempts have been made to covalently bind or graft CS onto man-made polymers or clays to strengthen its structure [9–29]. Such modification is not desirable because it may inadvertently alter CS properties, making it not biocompatible and toxic and lessening or removing its unique properties. A new method which can effectively *dissolve both CS and CEL* not at high temperature and not by corrosive and volatile solvents but rather by recyclable "green" solvent is particularly needed. This is because such method would facilitate preparation of [CEL+CS] composite material which is not only biocompatible but also has combined properties of its components, namely mechanical strength (from CEL) and hemostasis, wound healing, bactericide, drug delivery and pollutant removal (from CS). Such demand makes recent report on ability of a simple ionic liquid, butyl methylimmidazolium chloride to dissolve up to 10% (w/w) of CEL, particularly important [36].

Butyl methylimmidazolium chloride ([BMIm$^+$Cl$^-$]) belongs to a group of compounds known as ionic liquids (ILs). ILs are organic salts that are liquid at room temperature [37–40]. They have unique chemical and physical properties, including being air and moisture stable, a high solubization power, and virtually no vapor pressure [37–40]. Because of these properties, they can serve as a "*GREEN.*" recyclable alternative to the volatile organic compounds that are traditionally used as industrial solvents [37–40]. Due to their

advantages, ILs have been used for applications which are not possible with other chemicals. For example, as described above, IL such as [BMIm$^+$Cl$^-$] can dissolve up to 10% (w/w) of CEL. This discovery is of particular significance as it makes it possible for the first time that CEL can be dissolved, regenerated and chemically modified by use of a simple and green solvent which has high solubility power and low toxicity. Recently, it was found that [BMIm$^+$Cl$^-$] can also dissolve CS as well [40].

The information presented is indeed provocative and clearly indicate that it is possible to develop a novel and green method to prepare novel polysaccharide composite materials for effective adsorption and removal of MCs. Such considerations prompted us to initiate this study which aims to hasten the breakthrough by systematically and revolutionarily exploit advantages of IL, a green solvent, to develop a novel, simple, pollution-free and ***recyclable method*** to dissolve ***both CEL and CS***, without using any harmful, volatile organic solvents and/or strong acid and base, for the preparation of polysaccharide ecocomposite materials containing CEL and CS, and to demonstrate that these materials are not only fully biocompatible but also superior to currently available materials for removal of MCs. The results of our initial investigation are reported herein.

2. MATERIALS AND METHODS

Chemicals

Microcrystalline CEL (Avicel, DP≈ 300 [41]), amorphous CEL and chitosan (MW≈310–375kDa, 75% degree of deacetylation, Sigma-Aldrich), microcystin-LR (Enzo Life Sciences) were used as received. 1-methylimidazole and 1-chlorobutane (Alfa Aesar) were further purified by distillation. [BMIm$^+$ Cl$^-$] was synthesized from 1-chlorobutane and 1-methylimidazole using method previously reported [42, 43]. This IL is known to be hygroscopic and because any water presence is known to decrease its ability to dissolve polysaccharides [44], the IL was dried under vacuum at 70°C overnight before use.

Instruments

UV-visible spectra were measured on a Perkin Elmer Lambda 35 UV/VIS spectrometer. NIR spectra were taken on a home-built NIR spectrometer based on an acoustooptic tunable filter. Information on this NIR spectrometer was described in detail in our previous papers [45, 46]. Normally, each spectrum was an average of 30 spectra taken at 1-nm intervals from 1450 to 2450 nm. FTIR spectra were measured on a PerkinElmer 100 spectrometer at 2 cm^{-1} resolution with either KBr or by a ZnSe single reflection ATR accessory (Pike Miracle ATR). Each spectrum was an average of 64 spectra. X-ray diffraction (XRD) measurements were taken on a Rigaku MiniFlex II diffractometer utilizing the Ni filtered Cu Kα radiation (1.54059Å). The voltage and current of the X-ray tube were 30kV and 15mA respectively. The samples were measured within the 2θ angle range from 2.0 to 40.0°. The scan rate was 5° per minute. Data processing procedures were performed with the Jade 8 program package [47]. Scanning electron microscopic images of surface and cross section of the polysaccharide composite materials were taken under vacuum with an accelerated voltage of 3 kV using Hitachi S4800 scanning electron microscope (SEM). Tensile strength measurements were performed on an Instron 5500R Tensile Tester.

Preparation of CEL, CS and [CEL+CS] composite films

Scheme 2 summarizes procedure used to dissolve and to regenerate films of CEL and/or CS with [BMIm$^+$Cl$^-$] as solvent. Specifically, CEL and/or CS were dissolved in [BMIm$^+$Cl$^-$] under argon and magnetic stirring at 100 – 110 °C. All polysaccharides were added in portions of approximately 1 wt% of the IL. Succeeding portions were only added after the previous addition had completely dissolved until the desired concentration has been reached.

For composite films, the components were dissolved one after the other, with CEL being dissolved first. Using this procedure, solutions of CEL (containing up to 10% w/w (of IL)), CS (up to 4% w/w) and composite solutions containing CEL and CS in various proportions were prepared in about 6–8 hours.

Upon complete dissolution, the homogeneous solutions of the polysaccharides in [BMIm$^+$ Cl$^-$] were cast on glass slides or Mylar sheets using a RDS stainless steel coating rod with appropriate size (RDS Specialties, Webster, NY) to produce thin films with different compositions and concentrations of CEL and CS. They were then kept at room temperature for 24 hours to allow the solutions to undergo gelation (henceforth referred as **Gel Films**).

In addition to the polysaccharides, the Gel Films also contained [BMIm$^+$Cl$^-$]. The IL was removed from the films by washing the films in water for 3 days to yield "[BMIm$^+$Cl$^-$]-free" films (i.e., **Wet Films**). During this period, the washing water was constantly replaced with fresh water to maximize the removal of the IL. The [BMIm$^+$Cl$^-$] used was recovered from the washed aqueous solution by distillation. Finally, **Dried Films** were obtained when the Wet Films are allowed to dry. Drying of the **Wet Films** was carried out at room temperature in a chamber with humidity controlled at 60%. Drying time was found to be dependent on thickness of the films but generally was in range of 2–3 days.

Detailed information on measurements of swelling, adsorption and desorption can be found in the Supplementary Data

3. RESULTS AND DISCUSSION

3.1 Synthesis and Characterization of [CEL+CS] Composites

Images of CEL, CS and [CEL+CS] composite materials during various stages of preparation are presented in Scheme 2. Specifically, images of films of one-component (CEL or CS) and two component [CEL+CS] casted right after the polysaccharides were dissolved in [BMIm$^+$Cl$^-$], i.e., **Gel Film**, are shown in top center-left of the Scheme. After soaking in water for 3 days, [BMIm$^+$Cl$^-$] was removed from the gel film to yield corresponding **Wet Films**. Finally, **Dried Films** were obtained when the wet film was allowed to dry at room temperature.

XRD, FTIR, NIR and ^{13}C Cross polarization-magic angle spinning NMR (CP-MAS-NMR) were used to follow and confirm the dissolution process and to characterize the films. Specifically, dissolution of CEL and CS in [BMIm$^+$Cl$^-$] was confirmed by XRD technique. Shown in Figure 1A are XRD spectra of microcrystalline CEL (pink curve), the CEL one-component **Gel Film** (orange curve), the corresponding **Dried Film** (green curve) as well as that of [BMIm$^+$Cl$^-$](blue curve) for reference . As illustrated, microscrystalline CEL exhibits diffraction peaks at $2\theta = 14.7°$ and $16.3°$, $22.5°$ and $34.6°$ for (101), (002) and (040) plane, respectively. These bands disappeared completely when the powder polysaccharide was dissolved in [BMIm$^+$Cl$^-$]. The disappearance of these bands together with the similarity between the spectrum of liquid [BMIm$^+$Cl$^-$] and that of the **Gel Film** clearly indicate that [BMIm$^+$Cl$^-$] completely dissolved the polysaccharide. Similar results were also found for CS (Figure 1B), namely, the fact that diffraction bands of the CS powder disappeared when they were dissolved in [BMIm$^+$Cl$^-$], clearly indicate that the [BMIm$^+$Cl$^-$] also completely dissolved this polysaccharide. Similar results were also obtained (Fig 1C) for two-component composite films containing [CEL+CS] of 10:3.

Recently, there have been some reports on toxicity of ILs. However, the IL used in this work, [BMIm$^+$Cl$^-$], is relatively nontoxic compared to other ILs (its EC-50 and LD$_{50}$ values are 897.47 ppm and 550mg/kg, respectively [48]). Nevertheless, it is desirable to completely

remove the IL from regenerated polysaccharide films to ensure the films are biocompatible. Since [BMIm$^+$ Cl$^-$] is totally miscible with water (the logP, its octanol-water partition coefficient, is - 2.4 [49]), it was removed from the **Gel Films** by washing the films with water. Washing water (2L for a composite film of about 10cm×10cm) was repeatedly replaced with fresh water every 24 hrs until it was confirmed that IL was not detected in the washed water (by monitoring UV absorption of the IL at 290 nm). It was found that after washing for 72 hours, no IL was detected in the washing water by UV measurements. Since the limit of detection of the spectrophotometer used in this work was estimated to be about 3×10^{-5} AU, and the molar absorptivity of [BMIm$^+$Cl$^-$] at 290 nm is 2.6 M^{-1}cm^{-1}, it is estimated that if any [BMIm$^+$Cl$^-$] remains, its concentration would be smaller than 2 μg/mL of the washed water and 2 μg/g of the composite film. Since this concentration is two orders of magnitude lower than the LD$_{50}$ value of the [BMIm$^+$Cl$^-$], if any IL remains in the composite films, it would not pose any harmful effect. UV-vis, FTIR and NIR techniques were used to: (1) confirm that when the composite films were washed with water, [BMIm$^+$Cl$^-$] was removed from the films to a level not detectable by these techniques; and (2) determine chemical composition of composite materials. Shown in Figure 2A is NIR spectrum of [BMIm$^+$Cl$^-$]. As illustrated, overtone and combination bands of aliphatic C-H groups of the [BMIm$^+$Cl$^-$] can be clearly observed at 1388 nm and 1720 nm [50]. Since these bands are specific for [BMIm$^+$Cl$^-$], they can be used as indicators to determine if the IL is present. Also shown in Figure 2A are NIR spectra of **Gel Films** of CEL, CS and [CEL +CS]. Spectra of these **Gel Films** are very similar to that of [BMIm$^+$Cl$^-$] because the IL was the main component of these films. As shown in Figure 2B, After washing with water to remove the IL, and drying, **Dried Films** of one-component CEL and CS samples were found to exhibit NIR spectra drastically different from those of their **Gel Films** shown in Fig 2A (spectra of Dried Films are shown together with the spectrum of [BMIm$^+$Cl$^-$] for reference). The fact that NIR spectra of the **Dried Films** (Fig 2B) exhibit none of the indicator bands specific for [BMIm$^+$Cl$^-$] clearly indicates that washing with water effectively removed the IL from the films to a level which is not detectable by NIR technique. Further confirmation of removal of the ionic liquid from the films can also be seen in Figure 2C which shows FT-IR spectra of the same samples shown in 2B, namely, [BMIm$^+$Cl$^-$] and **Dried Films** of CEL and CS. As illustrated, [BMIm$^+$Cl$^-$] exhibits several distinct bands at around 756 cm^{-1}, 1173 cm^{-1}, 1468 cm^{-1} and 1572 cm^{-1}. These bands can be attributed to aromatic C-H bending, -C=N- stretching, aromatic C-H in-plane bending and aromatic C=C stretching, respectively [51, 52]. Again, none of these bands were present in the spectra of both CEL and CS **Dried Films** indicating that by washing with water, [BMIm$^+$Cl$^-$] was removed from the composite films to a level which is not detectable by FTIR method.

The IL used was recovered by distilling the washed aqueous solution (the IL remained because it is not volatile). The recovered [BMIm$^+$Cl$^-$] was dried under vacuum at 70°C overnight before reuse. If needed, recovered [BMIm$^+$Cl$^-$] was decolored by heating at 70°C with activated charcoal. *It was found that at least 88% of [BMIm$^\pm$Cl$^=$] was recovered for reuse*. **As such, the method developed here is recyclable because [BMIm$^+$Cl$^-$] is the only solvent used in the preparation and it is recovered for reuse.** FTIR and NIR results indicate that recovered [BMIm$^+$Cl$^-$] is structurally the same as freshly prepared[BMIm$^+$Cl$^-$], and that composite materials prepared using recovered [BMIm$^+$Cl$^-$] were found spectroscopically to be the same as those prepared using freshly made [BMIm$^+$Cl$^-$].

It is important to point out that the method developed here is not only different but also superior to the method recently reported in which magnetic CEL-CS gel microspheres were prepared using [BMIm$^+$Cl$^-$] as a solvent. This is because that method is not green (various chemicals including vacuum pump oil, Span 80, ethanol), not recyclable (used [BMIm$^+$Cl$^-$] is not recovered for reuse) and can only prepare microspheres [53, 54]. Conversely, the method developed here is green and recyclable (the only chemical used is [BMIm$^+$Cl$^-$] and

at least 88% of it was recovered for reuse) and can produce [CEL+CS] composite materials in various forms (e.g. thin films, microparticles) which make them particularly suited for various applications.

It is noteworthy to add that the cost of [BMIm$^+$Cl$^-$] is comparable to those of solvents traditionally used to dissolve CEL and CS (see, for example, prices quoted in Sigma-Aldrich catalog: USD105/50g of [BMIm$^+$Cl$^-$] compared to USD46/500 mL of acetic acid (for traditional dissolution of CS); USD225/100g of metylmorpholine and USD230/100g of dimethylthexysilyl chloride (for traditional dissolution of CEL)). *However, the method reported here is much more economical compared to other methods because [BMIm$^\pm$Cl$^=$] used in the dissolution is not lost but rather recovered for reuse*.

Analysis of the film materials by SEM reveals some interesting features about the texture and morphology of the materials. Shown in Figure 3 are surface (top three images) and cross section images (bottom three images) of regenerated one component CS film (left) and CEL film (right) as well as 50:50 CEL:CS composite film (middle images). As expected, both surface and cross section images clearly indicate that one-component CEL and CS are homogeneous. Chemically, the only difference between CS and CEL is the few –NH$_2$ groups in the former. However, their structures, as recorded by the SEM, particularly the cross section images, are substantially different. Specifically, while CS seems to exhibit smooth structure, CEL arranges itself into fibrous structure with fibers having diameter of about ~0.5–1.0 micron. As expected, the 50:50 CEL:CS composite material is not only homogeneous but also its structure is similar to both CEL and CS.

Chemically, the regeneration of both CEL and CS was confirmed by FTIR spectroscopy. As illustrated in figure 4A, the FTIR spectrum of microcrystalline CEL (blue spectrum) exhibits three pronounced bands at around 3400cm^{-1}, 2850–2900cm^{-1} and 890–1150cm^{-1}. These bands can be tentatively assigned to stretching vibrations of O-H, C-H and -O- group, respectively [55–57]. The fact that the **Dried Film** (red spectrum in 4A) also exhibits these three bands and is very similar to that of the microcrystalline CEL clearly indicates that CEL was completely regenerated by this synthetic method. Similarly, the FT-IR spectrum of a CS **Dried Film** (green spectrum in 4B) is similar to the FTIR spectrum of the CS powder (blue spectrum) from which it was made. These spectra display characteristic CS bands around 3400cm^{-1} (O-H stretching vibrations), 3250–3350cm^{-1} (symmetric and asymmetric N-H stretching), 2850–2900cm^{-1} (C-H stretching), 1657cm^{-1} (C=O, amide 1), 1595cm^{-1} (N-H deformation), 1380cm^{-1} (CH$_3$ symmetrical deformation), 1319cm^{-1} (C-N stretching, amide III) and 890 – 1150cm^{-1} (ether bonding) [55–57]. These results indicate that both CEL and CS were successfully regenerated by the synthetic method developed here without any chemical transformation.

Results from NIR measurements further confirm regeneration of polysaccharide composite materials. Shown in Figure 4C are NIR spectra of microcrystalline CEL and regenerated CEL **Dried Film** (4C) and CS powder together with regenerated CS **Dried Film** (4D). As illustrated in 4C, both CEL microcrystalline and regenerated CEL film exhibit bands around 1492nm, 1938nm and around 2104nm. These can be attributed to the overtone and combination transition of the –OH groups. Since CS also possesses the same O-H groups in addition to N-H$_2$ group, NIR spectra of CS powder and film (4D) also have additional bands at around 1548nm and 2028nm which expectedly can be attributed to the –NH modes [57–60]. The similarity between the NIR spectra of starting polysaccharides and regenerated polysaccharide further confirms that CEL and CS were successfully regenerated by this preparation method.

^{13}C CP-MAS-NMR technique was then employed to further confirm structure of regenerated polysaccharide composite materials. Shown in Figure 5 are ^{13}C CP-MAS-NMR spectra obtained for regenerated **Dried Films** of CEL (purple spectrum D), CS (red spectrum B) and 5:3 CEL:CS composite (light blue spectrum A) together CS powder (green spectrum C) amorphous cellulose powder (black spectrum E) and microcrystalline cellulose powder (dark blue spectrum F). Chemical shifts of all six samples are listed in Table 2. As expected, the spectra of CS powder, amorphous CEL powder and microcrystalline CEL powder agree with reported spectra [61–63]. The observed similarity between spectra and chemical shifts of corresponding carbons of regenerated dried films of CS and CEL to those of powder CS and powder of amorphous CEL is a clear indication that CEL and CS were successfully regenerated. Of particular interest is the fact that the spectrum of regenerated CEL film is similar to that of the amorphous CEL powder, and is distinctly different from that of microcrystalline powder. This can be clearly seen at band corresponding to C_4 which is only a broad single band at 83.9 ppm, 84.4 ppm, respectively for regenerated CEL and amorphous CEL, but a doublet at 88.7 ppm and 83.7 ppm for crystalline CEL powder. These results seem to indicate that when microcrystalline CEL was dissolved by and regenerated from the IL, the regenerated CEL has relatively lower crystallinity than the microcrystalline CEL because IL disrupted inter- and intramolecular hydrogen bond network during the dissolution process. As a consequence, the regenerated CEL adapts an amorphous structure. These results not only confirm conclusion based on XRD results presented in previous section but also are in agreement with other previous studies [61–63]. CEL has relatively different chemical shifts compared to those of CS, particularly C2 and C6; i.e., in CEL, a single C6 band is at 62.0 ppm, C2 is together with C3 and C5 in a large band at 74.1 ppm whereas in CS, C2 and C6 are together in a band at around 61.0 ppm, and the large band at 75.4 ppm is due only to C3 and C5. Since these bands can be resolved into individual bands corresponding to C2, C3, C5 and C6 for each CEL and CS component of composite materials, it is possible to determine concentration of each polysaccharide component in composite materials using the CP-MAS-NMR technique. Of particular interest is the presence of the band corresponding to carbon of CH_3 group in CS and CEL:CS composite material (but not in CEL) at around 22.7 ppm. This band can be attributed to remaining acyl groups of chitin, namely, chitosan obtained from commercial sources is not 100% but, as specified by the manufacturer in our case, is only >75% converted from chitin. In fact, by accumulating spectra for longer time, this CH_3 band can be clearly observed, and it can be used, together with FTIR method to determine exact degree of deacetylation of chitosan.

3.2 Properties of [CEL+CS] Composites

As described above, mechanical strength of CS is so poor that practically it cannot be used by itself for applications based on its unique properties. Measurements were made to determine tensile strength of pure CS film and (CS+CEL) composite films with different CEL concentrations in order to determine if by adding CEL into CS, the [CEL+CS] composite material would have adequate mechanical strength for practical applications. Results obtained, shown in Fig 6A, clearly indicate that adding CEL into CS substantially increase its tensile strength. For example, up to 5X increase in tensile strength can be achieved by adding 80% of CEL into CS, and that the tensile strength of the composite material can be adjusted by adding judicious amount of CEL. More importantly, the tensile strengths of [CS+CEL] composite materials are comparable with those of existing CS materials including those prepared by either grafting or copolymerization with other chemicals [64–69].

As described above, CS has relatively poor mechanical strength because it undergoes swelling in water. Adding CEL into CS was found to improve mechanical strength of the composite. However, since the [CEL+CS] composite still swell in water, it is important to

investigate the swelling of [CEL+CS] composites with different compositions in order to determine the optimal CEL/CS ratio which, in spite of swelling, can still provide a composite with adequate mechanical strength for its utilization. Accordingly, kinetics of swelling of [CEL+CS] composites with different compositions ranging from 0% to 100% CS were measured and results obtained are shown in Figure 6B which plot swelling ratio (S %) as a function of time. As illustrated, for all composites, the water swelling occurred rapidly, reaching equilibrium in water uptake at about 120 min. As expected, the swelling ratio was found to be proportional to the relative concentration of CS in the material with 100% CEL having the lowest value of 80% and 100% CS with the highest value of 270% . Values for other composites are between these two values. More quantitative assessment can be obtained from equilibrium water content (EWC(%) values. EWC % and tensile strength values for [CEL+CS] composites with different compositions from 0 to 100% CS are listed in Table 1 and plotted together, as a function of CEL in the composites (Figure 6A). It is evident from the figure that the relationship between the tensile strength with CEL concentration is opposite to that of the swelling, namely, increasing CEL concentration leads to the increase in the tensile strength and the decrease in the swelling. However, the relative increase in the tensile strength is much larger than the decrease in the swelling. For example, tensile strength of 100% CEL is 82.6 MPa which is 588% higher than that of 0% CEL (12.0 MPa) whereas its EWC% value of 46.4% is only 58% lower than the value for 73.6% for 0%CEL. This finding is particularly important because it clearly indicates that mechanical strength of the composite can be substantially strengthened by adding only relatively small amount of CEL. The composite still can retain its unique properties because the concentration of CEL added is so small to have any pronounced effect on the unique properties of the composites which are due solely to CS.

Taken together, results presented clearly indicate that we have successfully developed a novel, green and recyclable method to dissolve CEL and CS and to prepare biocompartible all polysaccharide composite materials containing CEL and CS. As anticipated, adding CEL to CS material substantially increases mechanical strength of the CS-based composite. It is expected that the [CEL+CS] composite may retain its unique properties including bactericide, fungicide, drug delivery as well as good adsorbent for pollutants and toxins (from CS). Initial evaluation of their ability to adsorb MC-LR is described in following section.

3.3 Adsorption of Microcystin-LR by [CEL+CS] Composites

Experiments were designed to determine: (1) if [CEL+CS] composite materials can adsorb MC; (2) if they can, mechanism of adsorption processes in terms of rate constants and adsorbed amounts at equilibrium; and (3) composite material which gives highest adsorption. These were accomplished by fitting kinetic data to both pseudo-first order and pseudo-second order models in order to determine appropriate reaction order for the adsorption processes based on R^2 and MSC values [70–72].

For pseudo-first order:

$$\ln(q_e - q_t) = \ln q_e - k_1 t \quad (1)$$

For pseudo-second order

$$\frac{t}{q_t} = \frac{1}{(k_2 q_e{}^2)} + \frac{t}{q_e} \quad (2)$$

where k_1 and k_2 are pseudo-first order and pseudo-second order rate constant of sorption (g/mg.min), q_e is the amount of analyte adsorbed at equilibrium (mg/g), q_t is the amount of analyte adsorbed at any time t (mg/g).

If the initial adsorption rate h is

$$h = k_2 q_e^2 \quad (3)$$

Then Eq 2 can be rearranged as

$$\frac{t}{q_t} = \frac{1}{h} + \frac{1}{q_e}t \quad (4)$$

A linear plot can be obtained by plotting t/q_t against t. q_e and h, can obtained from the slope and intercept; k_2 can be calculated from h and q_e according to Eq 3.

As described in experimental section, kinetics of adsorption of MC by composite materials were determined by measuring change (i.e., decrease) in absorbance at 238 nm as a function of time in a solution containing a composite film. From measured absorbances, the amount of adsorbed MC at time t (i.e., q_t) can then be calculated. Shown in figure 7A is plot of q_t as a function of time for six different [CEL+CS] materials with different composition ranging from 0% to 67% CS. It is evident from this plot that increasing CS concentration in the composite material led to increase in amount of microcystin adsorbed at equilibrium. Detailed information on adsorption kinetics can be obtained by fitting the data to both pseudo-first order (eq 1) and pseudo-second order (eq 4) model. Listed in Table 3 are results obtained for [CEL+CS] composite materials with different composition ranging from 20% to 67% of CS. It was found that 0% chitosan (i.e., 100% CEL) material does not adsorb MC, and adsorption by composite material with <20% CS was too small to be measured. Typical linearized plots for pseudo-1st order and psedo-2nd order for two samples are shown in Figure 8. It is evident from the plots as well as from the fact that R^2 and model selection criteria (MSC) values in all cases are relatively higher for pseudo-2nd order than for pseudo-1st order indicating that adsorption process follows pseudo-2nd order model. Results obtained clearly show that CS composite materials can adsorb MC very well. Material without CS (i.e., 0%CS or 100% CEL) does not adsorb MC at all (yellow curve in Figure 7A), and that up to 96 mg of MC can be adsorbed per g of the composites. The adsorptivity was found to be dependent on the concentration of CS in the composite, namely, increasing concentration of CS leads to an increase in amount of adsorbed MC. For example, increase of CS concentration from 20% to 67% led to 128% increase in the amount of adsorbed MC. This is as expected because adsorption is due mainly to CS; CEL does not have any adsorption ability toward MC. The role of CEL in the composite is, as explained above, to strengthen mechanical properties of the material. Again there is a concern that CS had two opposite effects on the properties of the composites: namely, it is responsible for the adsorption of MC but it also undergoes swelling in water which leads to weakening structure of the composites. However, this should not be a problem because the increase in adsorption efficiency with the CS concentration is much larger than that of the swelling (i.e., EWC %). Specifically, increase of CS concentration from 20% to 67% led to 128% increase in the amount of adsorbed MC but only 29.2% increase in swelling (from 54.1 to 69.9%).

As described in the introduction, currently there are several absorbents available for removal of MC. Table 4 summarizes some of more popular adsorbents together with amount (mg) of MC which can be removed per gram of the adsorbent. It is evidently clear from the table that the [CS+CEL] composite materials reported here is much better adsorbent than all other

materials. For example, one gram of the best reported adsorbent, $Fe_3O_4@SiO_2$ magnetic microspheres, can only adsorb 20 mg of MC whereas 1 g of the [67%CS+23%CEL] material can remove up to 96 mg or 4.8 times more MC.

Investigations were also carried out to determine if the [CEL+CS] composites can be reused after they adsorb MC. Shown in Figure 7B is plot of q_t as a function of time during adsorption and desorption process for four different [CEL+CS] materials with different compositions ranging from 0% to 67% CS (for clarity, plot is shown for only four composites) . Specifically, the early portion of the plot (from t=0 to t=24 hr) is the same as the plot of adsorption process shown in Figure 7A in which the composite materials adsorbed MC from solution. After 24 hrs, which was long after adsorption equilibrium had been reached, the composite materials were removed from the MC solutions and placed in pure water. This time, the MC previously adsorbed in the composite underwent desorption from the composites into the water (in both adsorption and desorption process, q_t values, which is the amount of MC in the composites at time t, were plotted. These values were calculated from measured concentrations of MC in solution). As illustrated, for all [CEL +CS] composites whose compositions ranging from 0 to 67% CS, MC previously adsorbed in the composites was quantitatively removed. These results clearly indicate that [CEL+CS] composites are not only very efficient adsorbents for MC but also that the adsorbed MC can be quantitatively desorbed to enable the composites to be reused.

Measurements were also performed to determine if there are any changes in adsorption capability of composite materials when the materials are reused for the second time, i.e., composite materials in which previously adsorbed MC are desorbed. Shown in Figure 9 are plot of q_t of adsorption of microcystin as a function of time by [CS+CEL] composite films containing 67%CS (A) and 50% CS (B). For comparison, two curves are shown for each composite: Blue curves are for 1st adsorption (i.e., by freshly prepared composites) and red curves are for 2nd adsorption (i.e., adsorption by composites that were regenerated by desorbing MC previously adsorbed). As illustrated, for both composites, adsorption capacity of the composite materials remains the same after they were regenerated by desorbing MC previously adsorbed.

4. CONCLUSIONS

In summary, we developed a simple and totally recyclable method to prepare biocompatible composites from CEL and CS. [BMIm$^+$Cl$^-$], an ionic liquid, was used as a solvent to dissolve and prepare the [CEL+CS] composite materials. Since the IL was removed from the composites by washing them with water, and recovered by distilling the washed solution, the method is totally recyclable. The [CEL+CS] composites were found to have combined advantages of their components, namely superior mechanical stability (from CEL) and excellent adsorption capacity for MC-LR, a deadly toxin produced by cyanobacteria (from CS). Specifically, it was found that mechanical strength of the composites increased with CEL loading; e.g., up to 5X increase in tensile strength was achieved by adding 80% of CEL into CS. More importantly, the tensile strengths of the composites are comparable with those of existing CS-based materials including those prepared by either grafting or covalently attaching CS to man-made polymers. On the other hand, CS had two opposite effects on the properties of the composites: namely, it is responsible for the adsorption of MC but it also undergoes swelling in water which leads to weakening structure of the composites. However, this should not be a problem because the increase in adsorption efficiency with the CS concentration is much larger than that of the swelling (i.e., EWC %). Additionally, not only the [CS+CEL] composite material reported here is biocompatible but also it is much better adsorbent than all other adsorbents currently available. For example, one gram of the best reported adsorbent, $Fe_3)_4@SiO_2$ magnetic microspheres, can only adsorb 20 mg of MC

whereas 1 g of the [67%CS+23%CEL] material can remove up to 96 mg of MC (i.e., 4.8X more than the magnetic microspheres). More importantly, not only that the MC adsorbed on the composite materials can be quantitatively desorbed to enable the [CS+CEL] composite material to be reused, but that adsorption capability of the reused composites remain the same as those used for the first time. Preliminary results presented in this study are very encouraging and clearly indicate that higher adsorption efficiency can be obtained by judiciously modifying experimental conditions (e.g., replacing films of composite with microparticles to increase surface area, and pH of solution). These possibilities are subject of our current intense study.

Supplementary Material

Refer to Web version on PubMed Central for supplementary material.

Acknowledgments

Appendix A

Supplementary data Supplementary data associated with this article can be found, in the online version, at

REFERENCES

1. See for examples, Svircev Z, Krstic S, Malidinov-Mikov M, Baltic V, Vidovic M. Freshwater Cyanobacterial Blooms and Primary Liver Cancer Epidemiological Studies in Serbia. J. Environ. Sci. Health C. 2009; 27:36–55. Giannuzzi L, Sedan D, Echenique R, Andrinolo D. An Acute Case of Intoxication with Cyanobacteria and Cyanotoxins in Recreational Water in Salto Grande Dam, Argentina. Mar. Drugs. 2011; 9:2164–2175. [PubMed: 22163179] Zegura B, Straser A, Filipic M. Genotoxicity and potential carcinogenicity of cyanobacterial toxins – a review. Mutation Res. 2011; 727:16–41. [PubMed: 21277993] Pearson L, Mihali T, Moffitt M, Kellmann R, Neilan B. On the Chemistry, Toxicology and Genetics of the Cyanobacterial Toxins, Microcystin, Nodularin, Saxitoxin and Cylindrospermopsin. Mar. Drugs. 2010; 8:1650–1680. [PubMed: 20559491]

2. Newcombe G, Nicholson B. Water Treatment options for Dissolved Cyanotoxins. J. Water Suppl. Res. Tech. 2004; 534:227–239.

3. Westrick JA, Szlag DC. A Review of Cyanobacteria and Cyanotoxins Removal/Inactivation in Drinking Water Treatment. Anal. Bioanal. Chem. 2010; 397:1705–1714. [PubMed: 20502884]

4. Chen L, Dionysiou DD, O'Shea K. Complexation of Microcystins and Nodularin by Cyclodextrins in Aqueous Solution, a Potential Removal Strategy. Environ. Sci. Tech. 2011; 45:2293–2300.

5. Finkenstadt VL, Millane RP. Crystal Structure of *Valonia* Cellulose 1β. Macromolecules. 1998; 31:7776–7783.

6. Augustine, AV.; Hudson, SM.; Cuculo, JA. Cellulose Sources and Exploitation. New York: Ellis Horwood; 1990.

7. Dawsey, TR. Cellulosic Polymers, Blends and Composites. New York: Carl Hanser Verlag; 1994.

8. Kadowaka M, Mukarami J, Kaneko Y. A facile preparation of gel materials from a solution of cellulose in ionic liquid. Carbohydrate Res. 2008b; 343:769–772.

9. Cai J, Liu Y, Zhang L. Dilute solution properties of cellulose in LiOH/urea aqueous system. J. Polym. Sci. B. Pol. Phys. 2006; 44:3093–30105.

10. Fink HP, Weigel P, Purz HJ, Ganster J. Structure formation of regenerated cellulose materials from NMMO-solutions. Progress Polym. Sci. 2001; 26:1473–1524.

11. Dai T, Tegos GP, Barkatovskaya M, Castano AP, Hamblin MR. Chitosan Acetate bandage as a topical antimicrobial dressing for infected burns. Anticrobial Agents Chemo. 2009; 53:393–400.

12. Bordenave N, Grelier S, Coma V. Hydrophobization and Antimicrobial activity of chitosan and paper-based packaging materials. Biomacromolecules. 2010; 11:88–96. [PubMed: 19994882]

13. Rabea EI, Badawy MET, Stevens CV, Smagghe G, Steurbaut W. Chitosan as antimicrobial agent: Applications and mode of action. Biomacromolecules. 2003; 4:1457–1465. [PubMed: 14606868]

14. Altiok D, Altiok E, Tihminlioglu F. Physical, antibacterial and antioxidant properties of chitosan films incorporated with thyme oil for potential wound healing applications. J. Mater. Sci: Mater. Med. 2010; 21:2227–2236. [PubMed: 20372985]

15. Burkatovskaya M, Tegos GP, Swietlik E, Demidova TN, Castano AP, Hamblin MR. Use of chitosan bandage to prevent fatal infections developing from highly contaminated wounds in mice. Biomaterials. 2006; 27:4157–4164. [PubMed: 16616364]

16. Gustafson SB, Fulkerson P, Bildfell R, Aguilera L, Hazzard TM. Chitosan dressing provides hemostasis in swine femoral arterial injury model. Prehospital Emergency Care. 2007; 11:172–178. [PubMed: 17454803]

17. Pusateri AE, McCarthy SJ, Gregory KW, Harris RA, Cardenas L, McManus AT, Goodwin CW. Effect of a chitosan-based haemostatic dressing on blood loss and survival in a model of severe venous hemorrhage and hepatica injury in swine. J. Trauma Injury Infect. Crit. Care. 2003; 54:177–182.

18. Keong LC, Halim AS. In vitro models in biocompatibility assessment for biomedical-grade chitosan derivatives in wound management. International J. Mol. Sci. 2009; 10:1300–1313.

19. Kiyozumi T, Kanatani Y, Ishihara M, Saitoh D, Shimizu J, Yura H, Suzuki S, Okada Y, Kikuchi M. Medium (DMEM/F12)-containing chitosan hydrogel as adhesive and dressing in autologous skin grafts and accelerator in the healing process. J. Biomed. Mat. Res. B: Appl. Biomat. 2006; 79B:129–136.

20. Rossi S, Sandri G, Ferrari F, Benferonic MC, Caramella C. Buccal delivery of acyclovir from films based on chitosan and polyacrylic acid. Pharm. Dev. Tech. 2003; 8:199–208.

21. Jain D, Banerjee R. Comparison of ciprofloxacin hydrochloride-loaded protein, lipid, and chitosan nanoparticles for drug delivery. J. Biomed. Mat. Res. B Appl Biomater. 2008; 86:105–112.

22. Varshosaz J, Tabbakhian M, Salmani Z. Designing of a thermosensitive chitosan/poloxamer in situ gel for ocular delivery of ciprofloxacin. Open Drug Delivery J. 2008; 2:61–70.

23. Elmotasem H. Chitosan-alginate blend films for the transdermal delivery of meloxicam. Asian J. Pharm. Sci. 2008; 3:12–29.

24. Naficy S, Razal JM, Spinks GM, G. G. Wallace GG. Modulated release of dexamethasone from chitosan-carbon nanotube films. Sensors Attuators A. 2009; 155:120–124.

25. Tirgar A, Golbabaei F, Hamedi J, Nourijelyani K, Shahtaheri SJ, Moosavi SR. Removal of airborne hexavalent chromium mist using chitosan gel beads as a new control approach. Int. J. Environ. Sci. Tech. 2006; 3:305–313.

26. Nishiki M, Tojima T, Nishi N, Sakairi N. β-Cyclodextrin-linked chitosan beads: preparation and application to removal of bisphenol A from water. Carbohydrate Lett. 2000; 4:61–67.

27. Hassan MAA, Hui LS, Noor ZZ. Removal of boron from industrial wastewater by chitosan via chemical precipitation. J. Chem. Nat. Res. Eng. 2009; 4:1–11.

28. Dhakal RP, Oshima T, Baba Y. Synthesis of unconventional materials using chitosan and crown ether for selective removal of precious metal ions. World. Acad. Sci. Eng. Tech. 2009; 56:204–208.

29. Ngah WWS, Isa IM. Comparison study of copper ion adsorption on chitosan, Dowex A-1, and Zerolit 225. J. Appl. Pol. Sci. 1998; 67:1067–1070.

30. Govindan VS. Effect of chitosan on harvesting of algal biomass from stabilization pond effluents. Asian Env. 1985; 7:4.

31. Qiao J, Dong L, Hu Y. Removal of harmful algal blooms using activated fly ash-modified chitosan. Fres. Env. Bull. 2011; 20:764–772.

32. Wang Y, Zhuo S, Yang Y, Li N. Application of chitosan in removing algae by dissolved air flotation. Adv. Mat. Res. 2012:347–353. (Pt. 4, Renewable and Sustainable Energy), 1911-1916.

33. Zou H, Pan G, Chen H, Yan. Removal of cyanobacterial blooms in Taihu Lake using local soils. II. Effective removal of Microsystis aeruginosa using local soils and sediments modified by chitosan. Env. Pollution. 2006; 141:201–205.

34. Pan G, Zou H, Chen H, Yuan X. Removal of harmful cyanobacterial blooms in Taihu Lake using local soils. III. Factors affecting the removal efficiency and an in situ field experiment using chitosan-modified local soils. Env. Pollution. 2006; 141:206–212.

35. Yan Q, Yu Y, Feng W, Pan G, Chen H, Chen J, Yang B, Li X, Zhang X. Plankton community sucession in artificial systems subjected to cyanobacterial blooms removal using chitosan modified soils. Microb. Ecol. 2009; 58:47–55. [PubMed: 18777048]

36. Swatloski RP, Spear S, Holbrey JD, Rogers RD. Dissolution of cellulose in ionic liquids. J. Am. Chem. Soc. 2002; 124:4974–4975. [PubMed: 11982358]

37. El Seould OA, Koschella A, Fidale LC, Dorn S, Heinze T. Applications of ionic liquids in carbohydrate chemistry: A Window of opportunities. Biomacromolecules. 2007; 8:2629–2647. [PubMed: 17691840]

38. Pinkert A, Marsh KN, Pang S, Staiger MP. Ionic liquids and their interaction with cellulose. Chem. Rev. 2009; 109:6712–6728. [PubMed: 19757807]

39. Tran CD, Lacerda SHP. Determination of Binding Constants of Cyclodextrins in Room Temperature Ionic Liquids by Near-Infrared Spectrometry. Anal. Chem. 2002; 74:5337–5341. [PubMed: 12403590]

40. See, for examples, Han X, Armstrong DW. Ionic Liquids in Separations. Acc. Chem. Res. 2007; 40:1079–1086. [PubMed: 17910515] Tran CD. Ionic Liquids Applications: Pharmaceutical, Therapeutics and Biotechnology. ACS Symposium Series. 2010; 1038:35–54. Welton T. Room-Temperature Ionic Liquids. Solvents for Synthesis and Catalysis. Chem. Rev. 1999; 99:2071–2083. [PubMed: 11849019] Wasserscheid P, Welton T. Ionic Liquids in Synthesis. 2003Weinheim, GermanyWiley-VCH Tran CD. Ionic liquids for and by Analytical Chemistry. Anal. Lett. 2007; 40:2447–2464.

41. Battista OA, Smith PA. Microcrystalline Cellulose: The oldest polymer finds new industrial uses. Industrial and Eng. Chem. 1962; 54:20–29.

42. Tran CD, Lacerda SHP. Determination of Binding Constants of Cyclodextrins in Room Temperature Ionic Liquids by Near-Infrared Spectrometry. Anal. Chem. 2002; 74:5337–5341. [PubMed: 12403590]

43. Frez C, Diebold G, Tran CD, Yu S. Determination of Thermal Conductivities, Thermal Diffusivities, and Sound Speeds of Room Temperature Ionic Liquids by Transient Grating Technique. J. Chem. Eng. Data. 2006; 54:1250–1255.

44. Swatloski RP, Spear S, Holbrey JD, Rogers RD. Dissolution of cellulose in ionic liquids. J. Am. Chem. Soc. 2002; 124:4974–4975. [PubMed: 11982358]

45. Baptista MS, Tran CD, Gao GH. Near Infrared Detection of Flow Injection Analysis by Acousto-Optic Tunable Filter Based Spectrophotometry. Anal. Chem. 1996; 68:971–976. [PubMed: 8651488]

46. Tran CD, Kong X. Determination of Identity and Sequences of Tri- and Tetrapeptides by Near-Infrared Spectrometry. Anal. Biochem. 2000; 286:67–74. [PubMed: 11038275]

47. Duri S, Majoni S, Hossenlopp JM, Tran CD. Determination of Chemical Homogeneity of Fire Retardant Polymeric Nanocomposite Materials by Near-infrared Multispectral Imaging Microscopy. Anal. Lett. 2010; 43:1780–1789.

48. Docherty KM, Kulpa CF. Toxicity and antimicrobial activity of imidazolium and pyridinium ionic liquids. Green Chem. 2005; 7:185–189.

49. Ropel L, Belveze LS, K. Aki SNV, Stadtherr MA, Brennecke JF. Octanol–water partition coefficients of imidazolium-based ionic liquids. Green Chem. 2005; 7:83.

50. Tran CD, Lacerda SP, Oliveira D. Absorption of Water by Room- Temperature Ionic Liquids: Affect of Anions on Concentration and States of Water. Appl. Spectrosc. 2003; 57:152–157. [PubMed: 14610951]

51. Jeon Y, Sung J, Seo C, Lim H, Cheong H, Kang M, Moon B, Ouchi Y, Kim D. Structures of ionic liquids with different anions studied by Infrared vibration spectroscopy. J. Phys. Chem. B. 2008; 112:4735–4740. [PubMed: 18366215]

52. Seethalakshmi K, Jasmine Vasantha Rani E, Padmavathy R, Radha N. FTIR spectral analysis of imidazolium chloride. Int. J. Cur. Res. Rev. 2012; 4:31–36.

53. Liu Z, Wang H, Li B, Liu C, Jiang Y, Yu G, Mu X. Biocompatible magnetic cellulose-chitosan hybrid gel microspheres reconstituted from ionic liquids for enzyme immobilization. J. Mater. Chem. 2012; 22:15085–15091.

54. Liu Z, Wang H, Liu C, Jiang Y, Yu G, Mu X, Wang X. Magnetic cellulose-chitosan hydrogels prepared from ionic liquids as reusable adsorbents for removal of heavy metal ions. Chem. Comm. 2012; 48:7530–7532.

55. Da Roz AL, Leite FL, Pereiro LV, Nascente PAP, Zucolotto V, Oliveira ON, Carvalho AJF. Adsorption of chitosan on spin-coated cellulose films. Carbohydrate Pol. 2010; 80:65–70.

56. Dreve S, Kacso I, Bratu I, Indrea E. Chitosan-based delivery systems for diclofenac delivery: Preparation and characterization. J. Phys.: Conference Series. 2009; 182:1–4.

57. Burns, DA.; Ciurczak, EW. Handbook of Near-Infrared Analysis. New York: Marcell Dekker; 1992.

58. Ellis JW. Infra-red absorption by the N-H bond II in aryl, alkyl and aryl-alkyl amines. J. Am. Chem. Soc. 1928; 50:685–695.

59. Baptista MS, Tran CD, Gao GH. Near Infrared Detection of Flow Injection Analysis by Acousto-Optic Tunable Filter Based Spectrophotometry. Anal. Chem. 1996; 68:971–976. [PubMed: 8651488]

60. Tran CD, Kong X. Determination of Identity and Sequences of Tri- and Tetrapeptides by Near-Infrared Spectrometry. Anal. Biochem. 2000; 286:67–74. [PubMed: 11038275]

61. Zhang L, Ruan D, Gao S. Dissolution and regeneration of cellulose in NaOH/Thiourea aqueous solution. J. Pol. Sci. Part B: Polymer Physics. 2002; 40:1521–1529.

62. Mori T, Chikayama E, Tsuboi Y, Ishida N, Shisa N, Noritake Y, Moriya S, Kikuchi J. Exploring the conformationa; space of amorphous cellulose using NMR chemical shifts. Carbohydrate Polymers. 2012; 90:1197–1203. [PubMed: 22939331]

63. Sebe G, Ham-Pichavant F, Ibarboure E, Koffi ALC, Tingaut P. Supramolecular structure characterization of cellulose II nanowhiskers producued by acid hydrolysis of cellulose I substrates. Biomacromolecules. 2012; 13:570–578. [PubMed: 22260431]

64. Kiuchi H, Kai W, Inoue Y. Preparation and characterization of poly(ethylene glycol) crosslinked chitosan films. J.Appl. Polym. Sci. 2008; 107:3823–3830.

65. Khamhan S, Baimark Y, Chaichanadee S, Phinyocheep P, Kittipoom SW. Water Vapor Permeability and Mechanical Properties of Biodegradable Chitosan/Methoxy Poly(ethylene glycol)-b-Poly(ɛ-caprolactone) Nanocomposite Films. Internt'l. J. Polym. Anal. Charact. 2008; 13:224–231.

66. Alam R, Khan AM, Khan AR, Ghoshal S, Mondal MIH. Study on the Physico-mechanical Properties of Photo-cured Chitosan Films with Oligomer and Acrylate Monomer. J. Polym. Env. 2008; 16:213–219.

67. Liang S, Liu L, Huang Q, Yam LK. Preparation of single or doublenetwork chitosan/poly(vinyl alcohol) gel films through selectively cross-linking method. Carbohydrate Polym. 2009; 77:718–724.

68. Khan MA, Alam R, Noor F, Khan RA, Md. Rahman A. Modification and Characterization of Chitosan Films Using 3-trimethoxysilylpropyl methacrylate. J. Macrom. Sci., Part A: Pure and Applied Chemistry. 2009; 46:751–758.

69. Radhakumary C, Prabha DN, Reghunadhan CPN, Mathew S. Chitosancomb- graft-polyethylene glycol monomethacrylate-Synthesis, characterization, and evaluation as a biomaterial for hemodialysis applications. J. Appl. Polym. Sci. 2009; 114:2873–2886.

70. Ho YS, McKay G. The kinetics of sorption of divalent metal ions onto sphagnum moss peat. Wat. Res. 2000; 34:735–742.

71. Kumar KV, Sivanesan S. Pseudo second order kinetics and pseudo isotherms for malachite green onto activated carbon: Comparison of linear and non- linear regression methods. J. Hazardous Mat. B. 2006; 136:721–726.

72. Li Q, Sun L, Zhang Y, Qian Y, Zhai J. Characteristics of equilibrium, kinetics studies for adsorption of Hg(II) and CRVI) by polyaniline/humic acid composite. Desalination. 2011; 266:188–194.

73. Gao Y, Gao N, Gu J, Shen Y. S Wang, Adsorption of Microcystin-LR from Water with Iron Oxide Nanoparticles. Water Environ. Res. 2012; 84:562–568. [PubMed: 22876478]

74. Chen H, Lu X, Deng C, Yan X. Facile synthesis of uniform microsphere composed of magnetite core and copper silicate nanotube shell for removal of Microcystins in water. J. Phys. Chem. C. 2009; 113:21068–73.

75. Morris RJ, Williams DE, Luu HA, Holmes CFB, Andersen RJ, Calvert SE. The adsorption of microcystin-LR by natural clay particles. Toxicon. 2000; 38:303–308. [PubMed: 10665811]

76. Yan H, Gong A, He H, Zhou J, Wei Y. Adsorption of microcystins by carbon nanotubes. Chemosphere. 2006; 62:142–148. [PubMed: 15893800]

77. Lee J, Walker H. Effects of process variables and natural organic matter on removal of microcystin-LR by PAC-UF. Environ. Sci. Technol. 2006; 40:7336–7342. [PubMed: 17180986]

78. Pyo D, Moon D. Adsorption of Microcystin LR by activated carbon fibers. Bull. Korean Chem. Soc. 2005; 26:2089–92.

79. Deng YH, Qi DW, Deng C, Zhang XM, Zhao DY. Superparamagnetic high-magnetization microspheres with an $Fe_3O_4@SiO_2$ core and perpendicularly aligned mesoporous SiO2 shell for removal of Microcystins. Am. Chem. Soc. 2008; 130:28–29.

Highlights

A novel and recyclable synthetic method using an ionic liquid, a Green Solvent.

Ecocomposite materials were synthesized from cellulose (CEL) and chitosan (CS).

Adding CEL into CS substantially increases tensile strength of the composite.

The composite is much better adsorbent for cyanotoxins than other materials.

The composite can be reused because adsorbed microcystin can be desorbed.
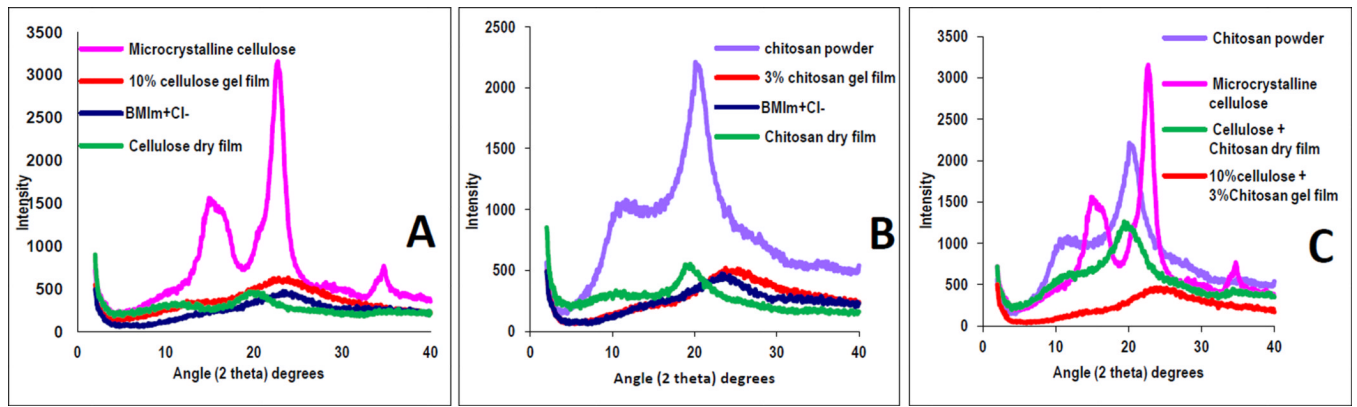
Figure 1.
XRD spectra of microcrystalline CEL, CS powder, regenerated CEL, CS and [CEL+CS] films.
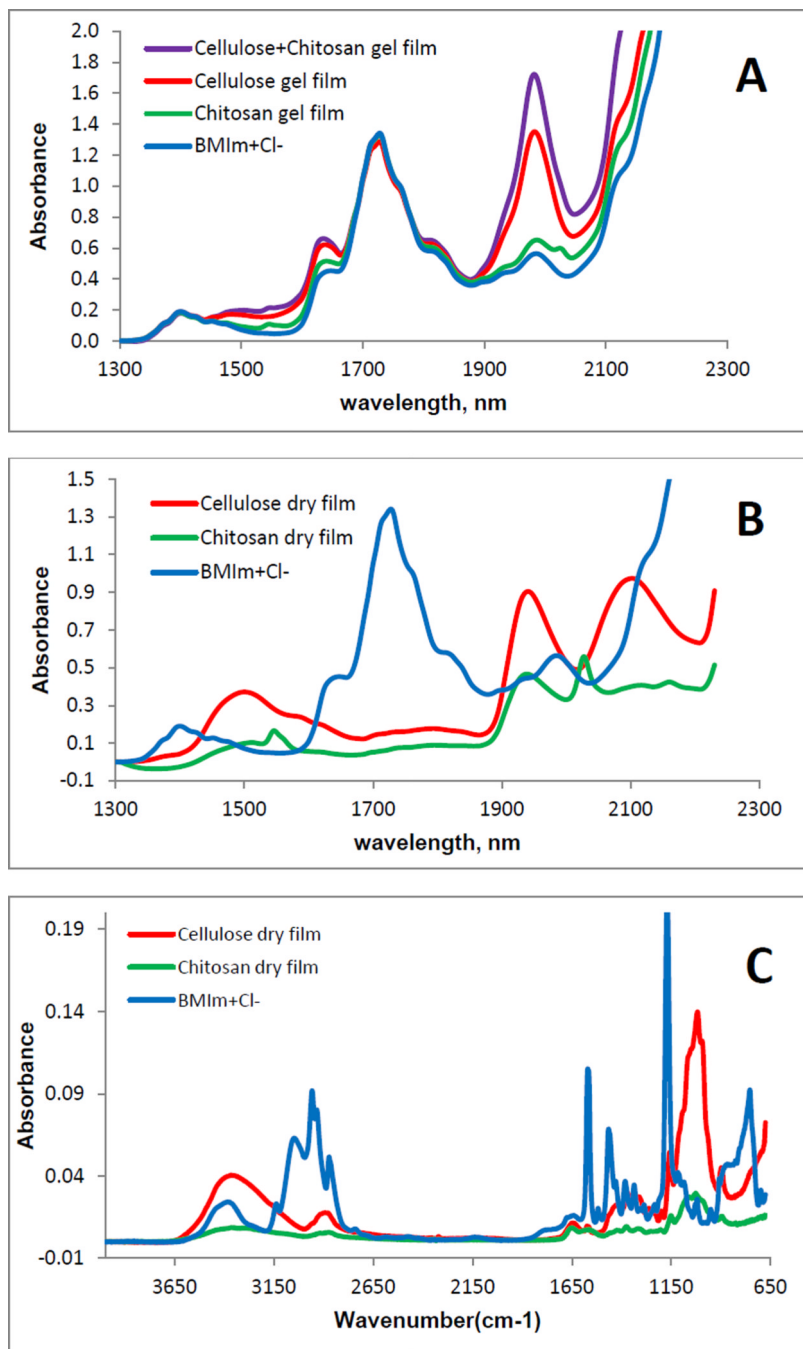
Figure 2.
NIR spectra (A and B) and FTIR spectra (C) of: **(A)**: [BMIm$^+$Cl$^-$] solution (blue), CEL Gel Film (red), CS Gel Film (green) and [CEL+CS] Gel Film; **(B)** [BMIm$^+$Cl$^-$] solution (blue), CEL Dried Film (red) and CS Dried Film (green); and **(C)** [BMIm$^+$Cl$^-$] solution (blue), CEL Dried Film (red) and CS Dried Film (green).
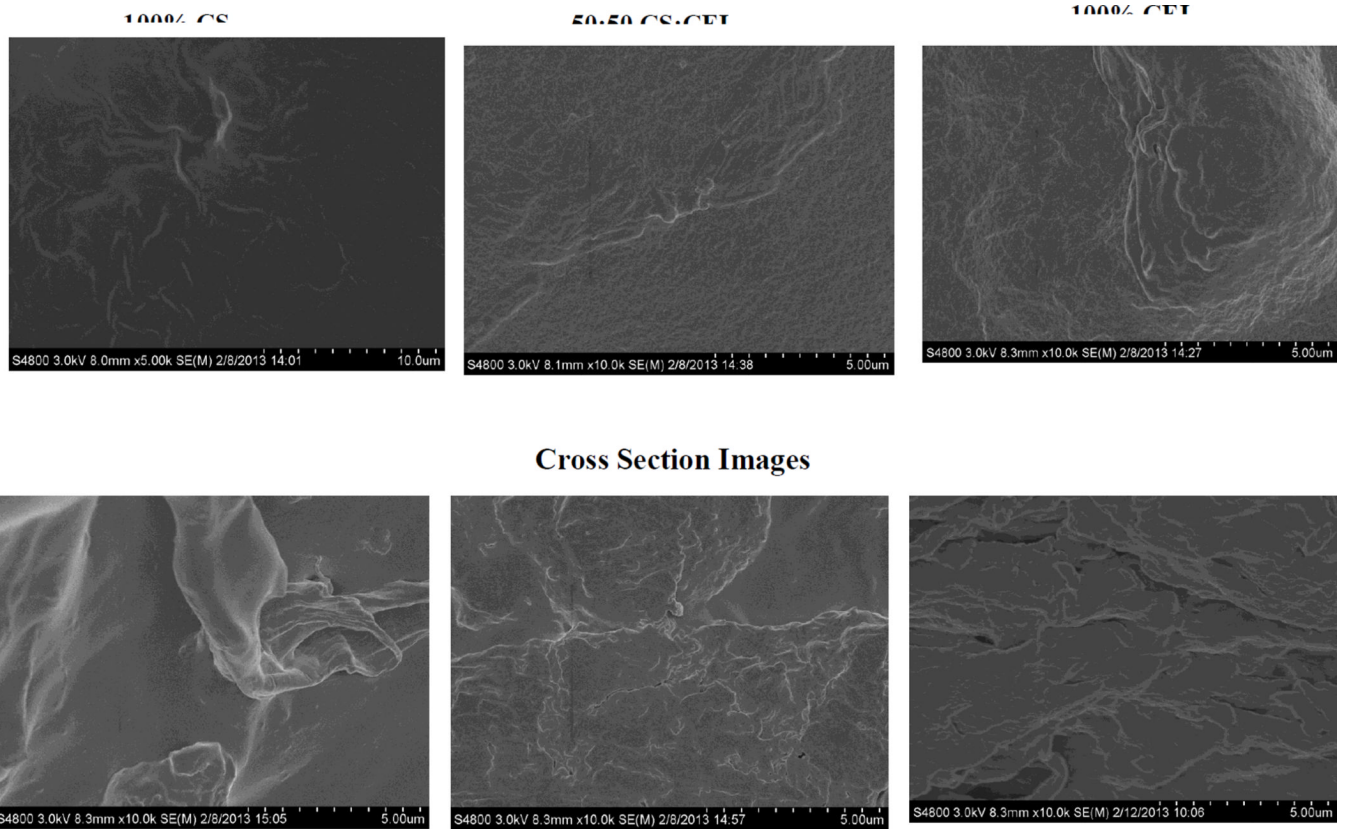
Figure 3.
SEM images of surface (top three images) and cross section (bottom three images) of regenerated CS film (left), regenerated CEL film (right) and 50:50 [CEL+CS] composite film (middle).
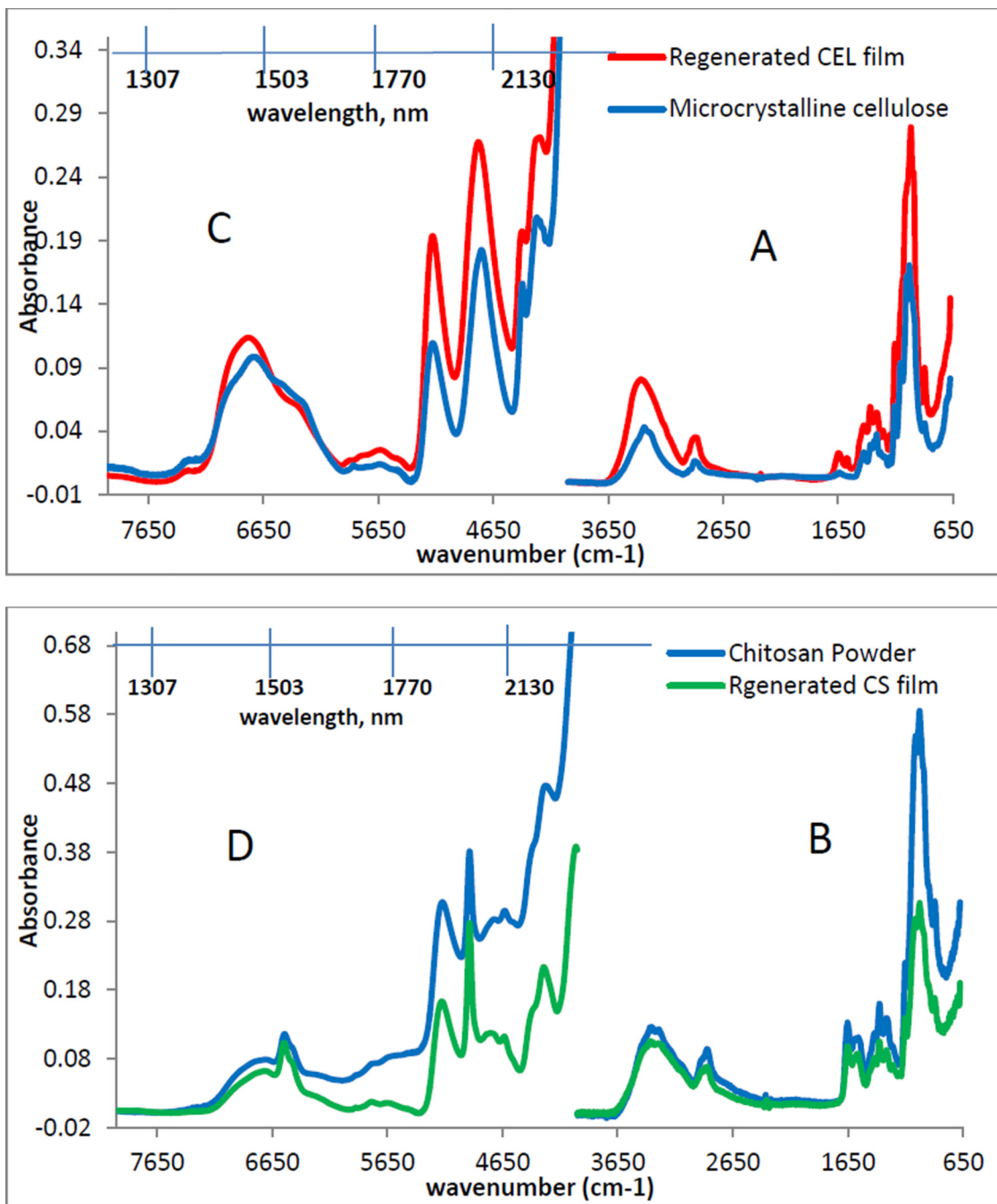
Figure 4.
FTIR spectra (A and B) and NIR spectra (C and D) of microcrystalline CEL (blue), regenerated CEL film (red), CS powder (blue) and regenerated CS film (green).
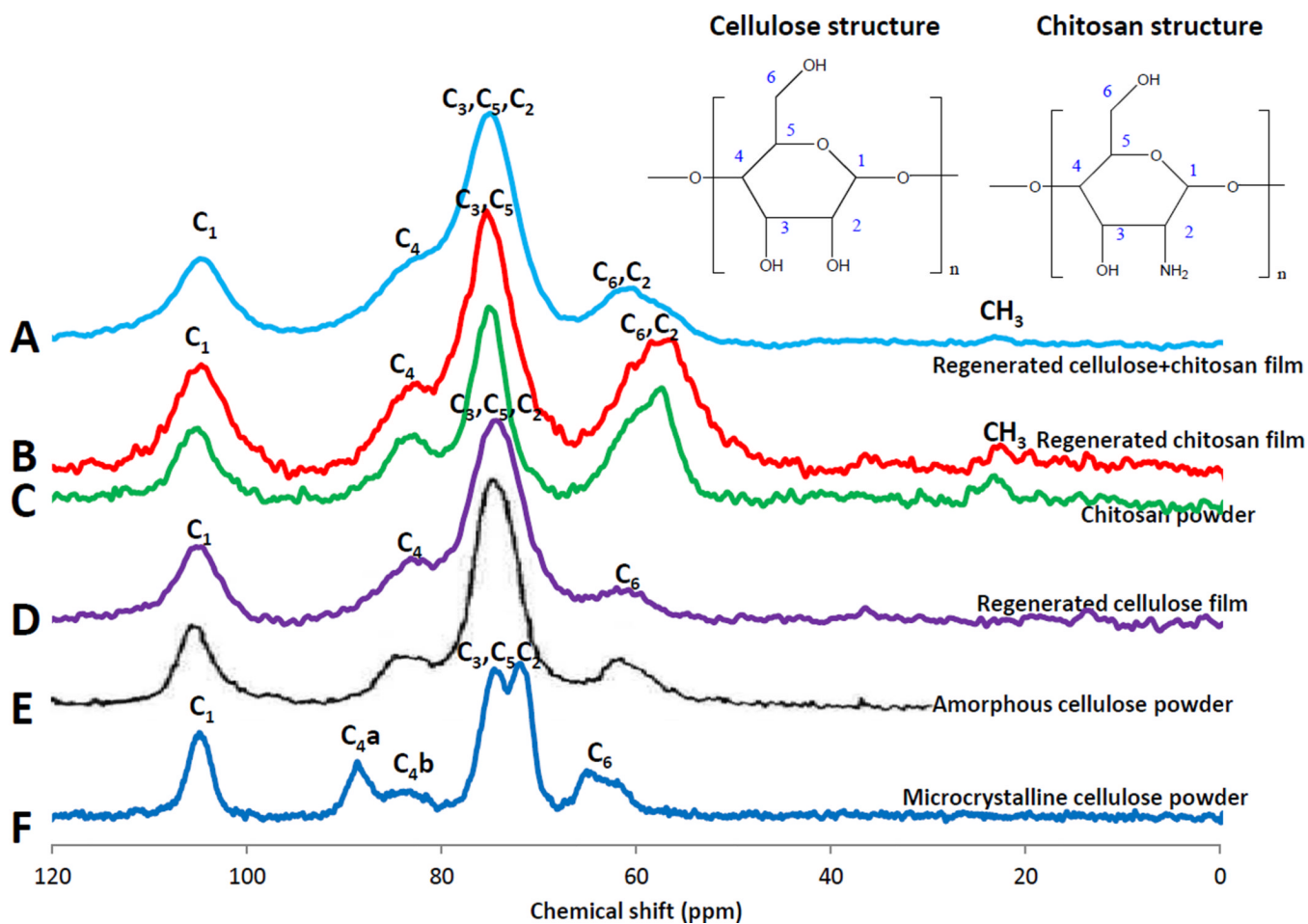
Figure 5.
^{13}C CP MAS NMR spectra of chitosan powder (C), amorphous CEL powder (E), microcrystalline CEL powder (F), regenerated CEL film (D), regenerated CS film (B) and [CEL+Cs] composite films (A).
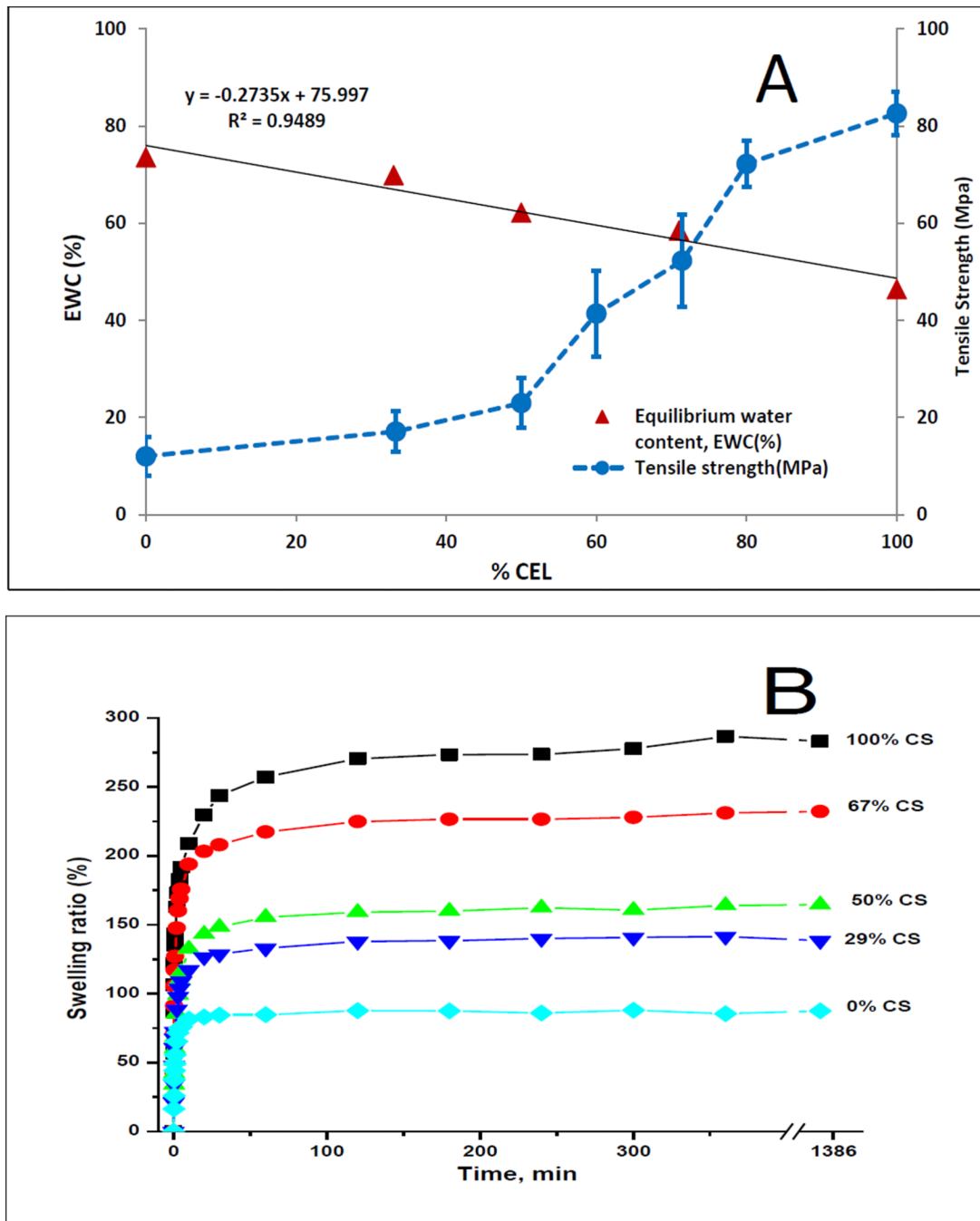
Figure 6.
(A) Plot of tensile strength and equilibrium water content (EWC%) as a function of CEL concentration and (B) swelling kinetics of different [CEL+CS] composite films.
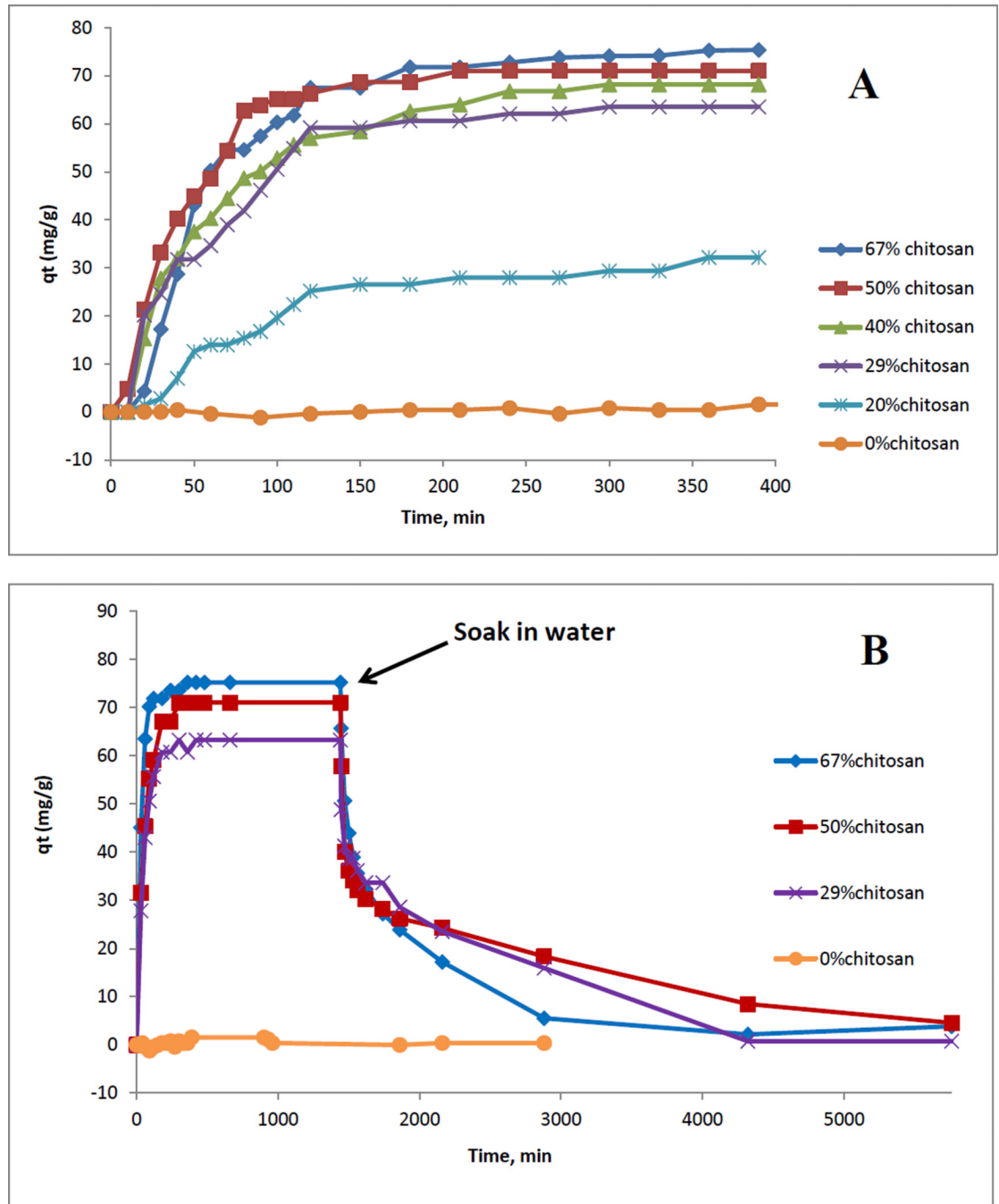
Figure 7.
Plot of q_t as a function of time for [CEL+CS] composite materials with different composition ranging from 20% to 67% CS.
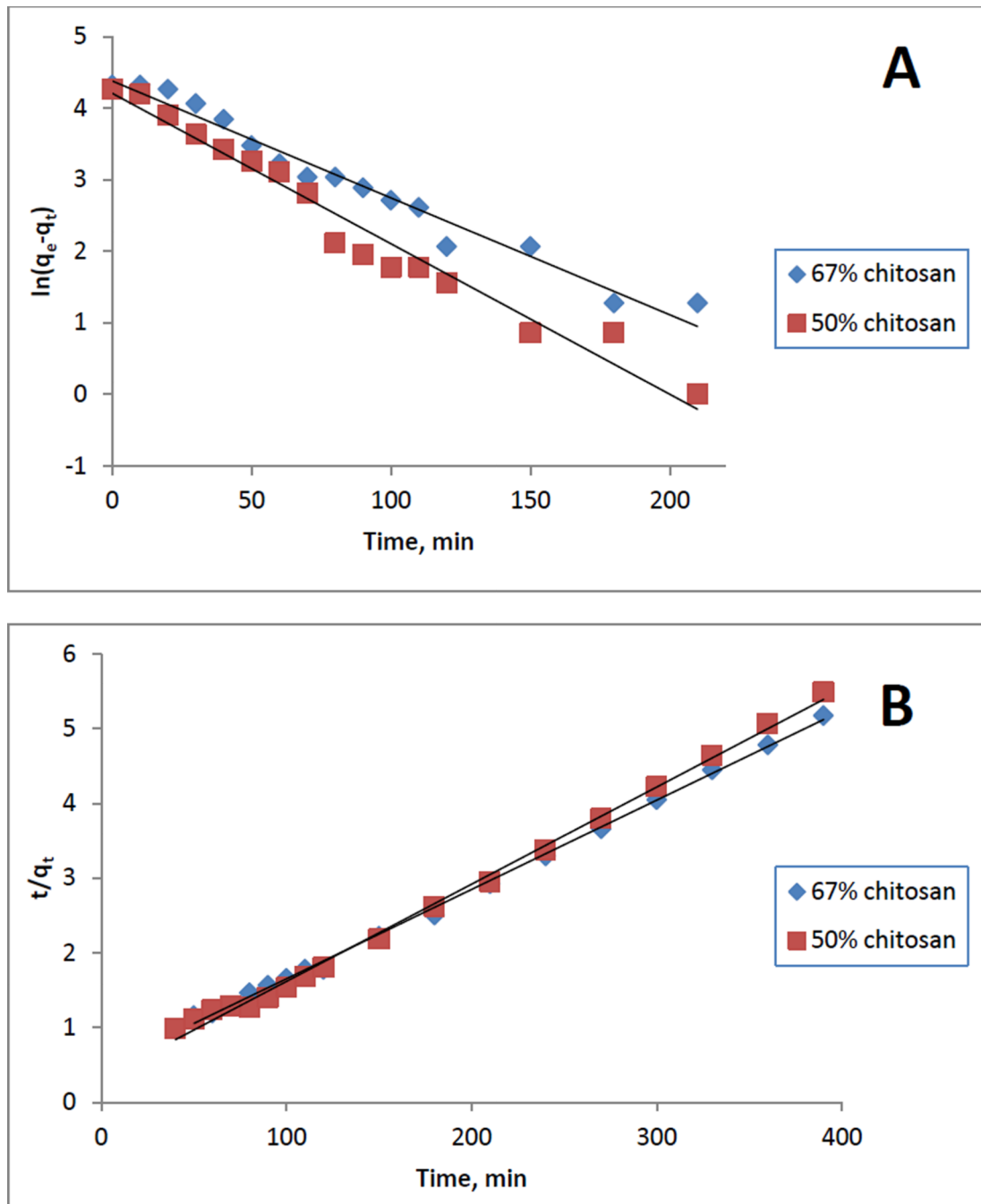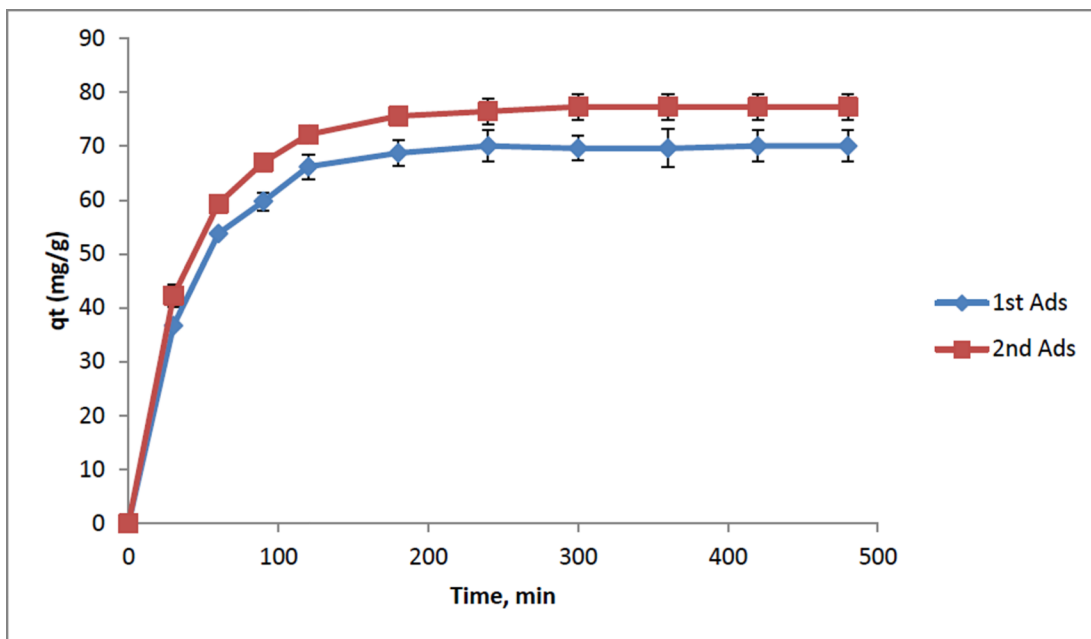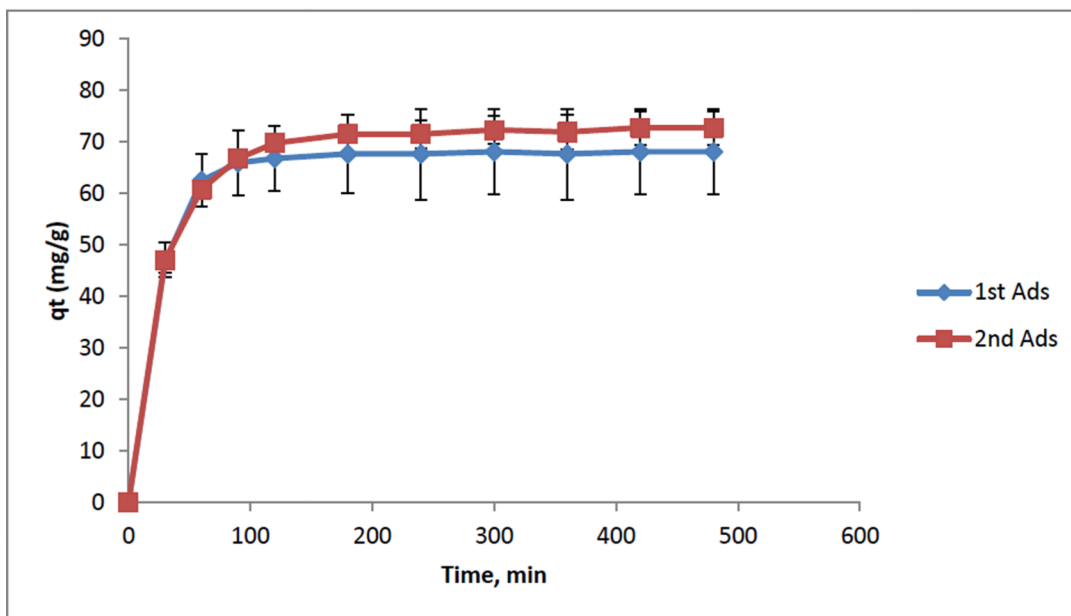
Figure 8.
Typical linearized plots for (A) pseudo-first order and (B) pseudo-second order models for [CEL+CS] composite films containing 67%CS and 50%CS
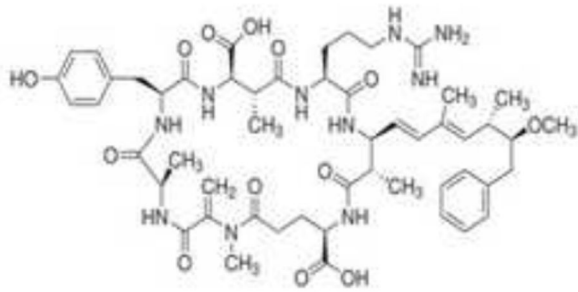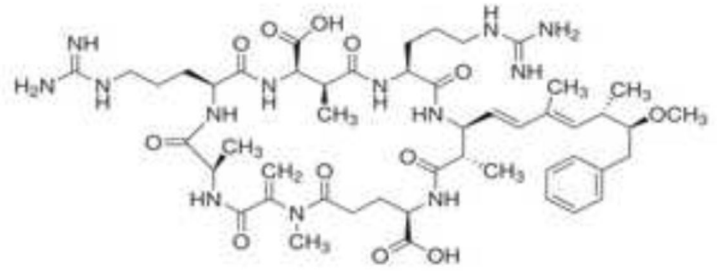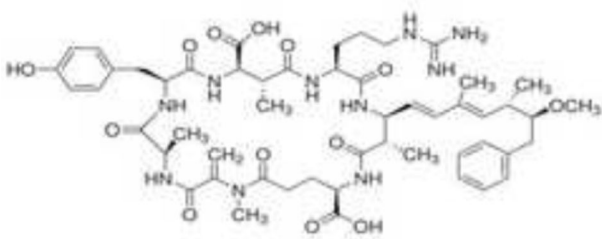
Figure 9.
Plot of q_t of adsorption of microcystin as a function of time by [CS+CEL] composite films containing 67%CS (A) and 50% CS (B): Blue curves are for 1st adsorption (i.e., by freshly prepared films) and red curves are for 2nd adsorption (i.e., adsorption by films that were regenerated by desorbing MC previously adsorbed).
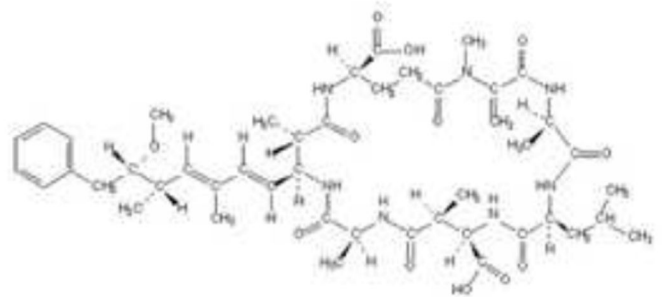
Microcystin LR
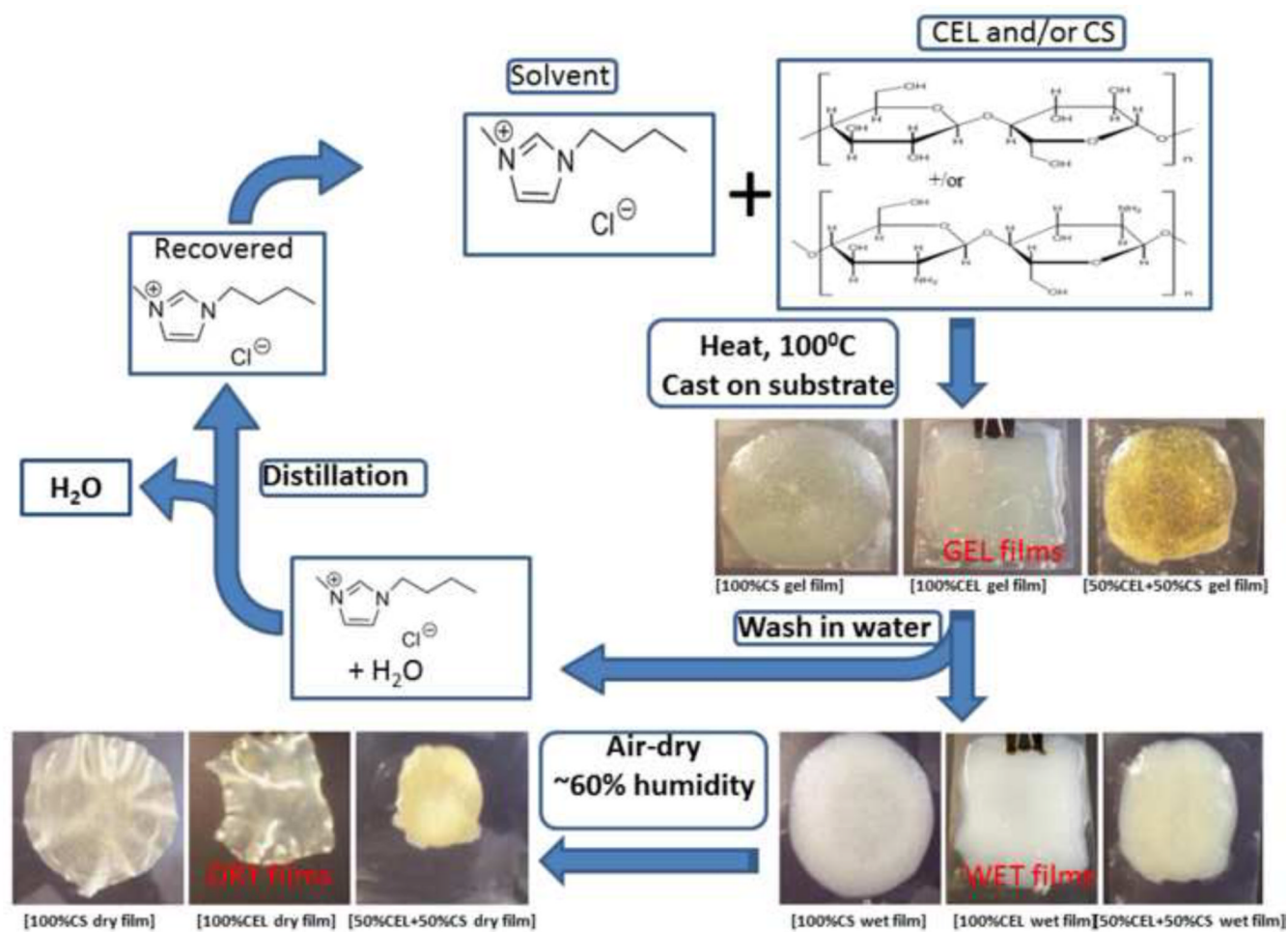

Microcystin RR

Microcystin YR

Microcystin LA

Scheme 1.
Structure of microcystins
(Note: nomenclature of the MCs is based on the amino acid substituents present, eg., L for leucine; R, arginine; Y, tyrosine; and A, alanine.)

Scheme 2.
Procedure used to prepare CEL, CS and [CEL+CS] composite materials.

Table 1

Tensile Strength and Swelling Parameters for [CEL+CS] Composites

%CS in [CEL+CS] composite	Tensile strength (MPa)	Equilibrium water content (EWC(%))
100	12.0	73.6
67	17.1	69.9
50	23	62.2
40	41.4	
29	52.3	58.5
20	72.2	
0	82.6	46.4

NIH-PA Author Manuscript

NIH-PA Author Manuscript

NIH-PA Author Manuscript

Table 2

^{13}C CP-MAS-NMR Chemical shifts of starting materials and regenerated CEL, CS and [CEL+CS] composite.

	Carbon chemical shifts (ppm)						
	C_1	C_2	C_3	C_4	C_5	C_6	CH_3
Regenerated cellulose film	104.6	74.1	74.1	83.9	74.1	62.0	
Amorphous cellulose powder	105.7	74.8	74.8	84.4	74.8	63.0	
Microcrystalline cellulose powder	104.9	72.1	74.6	83.7, 88.7	74.6	64.7, 62.3	
Regenerated chitosan film	104.7	61.0	75.4	83.6	75.4	61.0	22.7
Chitosan powder	104.9	60.1	74.7	84.0	74.7	60.1	23.4
Regenerated cellulose+chitosan film	104.5	56.4	75.5	83.9	75.5	61.5	23.0

Table 3

Parameters for Microcystin-LR Adsorption by [CEL+CS] Composites

| Composite Material | | Pseudo-First Order | | | | Pseudo-Second Order | | | |
% Chitosan	% Cellulose	Q_e (mg/g)	k_1 (min^{-1})	R^2	MSC	Q_e (mg/g)	$k_2 \cdot 10^4$ (g/mg. min)	R^2	MSC
67	33	94±8	0.020±0.001	0.9714	2.84	96±3	1.6±0.1	0.9894	4.18
50	50	72±1	0.02±0.01	0.9794	3.86	79±2	5±3	0.9953	5.46
40	60	52±1	0.010±0.007	0.9370	2.72	73±9	3±1	0.9965	5.66
29	71	44±1	0.01±0.02	0.9419	2.73	71±2	5±2	0.9987	6.52
20	80	31±5	0.007±0.001	0.7254	1.98	42±4	1.9±0.3	0.9932	5.00

Table 4

List of Adsorbents for MC-LR

Adsorber	mg of adsorbed MC-LR /g adsorber	Reference
Iron Oxide Nanoparticles	0.15	[73]
Fe$_3$O$_4$@copper silicate nanotube microspheres	0.5	[74]
Powdered activated carbon (PAC)	0.75	[2]
Natural clay particles	4.6	[75]
Carbon nanotubes	5.9	[76]
PAC/UF (membrane ultrafiltration)	9.9	[77]
Activated carbon fibers (ACF)	17	[78]
Fe$_3$O$_4$@SiO$_2$ magnetic microspheres	20	[79]
[CS+CEL] composite	96	This work